CHAPTER 7

OTHER BREAKWATERS

7-1. General. Protection for most coastal projects will probably be most advantageously provided by a structure of the rubble-mound, vertical wall or floating type; however, some projects may be best served by other unique structure types. It is beyond the scope of this manual to provide design guidance for all types of breakwaters. The pneumatic, hydraulic, and sloping float breakwaters have been chosen for inclusion herein, since they have generated more interest than most other lesser known structure types.

7-2. Pneumatic Breakwater System. The pneumatic breakwater concept was patented in 1907 (item 10). Wave attenuation is achieved by releasing compressed air through a submerged perforated pipe. Several prototype installations of this system have been described as successful. A few model studies were conducted prior to 1950, but the results were incomplete and in some cases contradictory.

a. Theoretical Analysis.

(1) Taylor conducted an analysis of the pneumatic breakwater, and his development became one of the most significant advances in this area of research (item 129). The investigation was formulated around the superposition of a uniform current of velocity, U, and thickness, h, on the velocity potential of a deepwater wave. It was assumed that air bubbles had little effect on the attenuation, and that the vertical current induced by the rising bubbles diffusing both upstream and downstream at the surface was solely responsible for the attenuation of the incident waves. Taylor's analysis was aimed at determining the current velocity necessary to attenuate waves of a given length, and he found that, for a given current, it was kinematically impossible to transmit waves shorter than a given length.

(2) Taylor modified the theory by using a triangular velocity distribution, which is more in accord with actual prototype distributions (item 130). To relate the velocity and thickness of the current to the air discharge and the submergence of the perforated pipe, the analogous solution for the convective currents above a horizontal line source of heat was used. The maximum velocity of the current U was found to be related to the air discharge q as

$$q = 0.00454U^3 \tag{7-1}$$

b. Small-Scale Experimental Studies. Several small-scale experimental studies conducted on pneumatic breakwaters (items 16, 36, 124, and 143) determined that the power required for discharging air through the pneumatic breakwater could be conveniently expressed by the dimensionless parameter

$$\Phi = \frac{(hp/ft)}{(\rho g^{3/2} L^{5/2})} \tag{7-2}$$

The horsepower per foot (hp/ft) at the orifices was computed from the expression

$$hp/ft = \frac{(q\gamma_w d_1)}{550} \tag{7-3}$$

where

ρ = density of water

g = acceleration of gravity

L = wavelength

q = unit air discharge at orifice

γ_w = unit weight of water

d_1 = submergences of orifices

(1) Effect of wave steepness. Wave steepness in the laboratory experiments varied from 0.02 to 0.08. It was found that the air requirement for a given attenuation was essentially independent of the wave steepness.

(2) Effect of orifice area. Straub, Bowers, and Tarapore investigated this effect with orifices of 1/8-, 3/16-, and 1/4-inch diameter (item 124). Test results indicated no pronounced change in the air requirements for the different orifice sizes.

(3) Use of multiple manifolds. Straub, Bowers, and Tarapore hypothesized that multiple parallel manifolds would be advantageous for attenuation of longer waves. This would provide a deeper surface current, thus enabling the breakwater to intercept the orbital motion over a greater part of the wavelength. Up to four manifolds were tested, but there appeared to be no advantage to using multiple manifolds. Actually, for lower discharges the airflow was not uniform and resulted in poor efficiency.

(4) Power requirement. For illustrative purposes, the horsepower required for a potential prototype installation was computed based on results of small-scale laboratory experiments of (item 124). Assuming an

installation depth of 40 feet and for various periods (wavelengths), attenuation as a function of applied horsepower per foot of breakwater is shown in figure 7-1. From this direct extrapolation of small-scale experimental data to prototype scale, it appears that the horsepower requirement would make operation very costly.

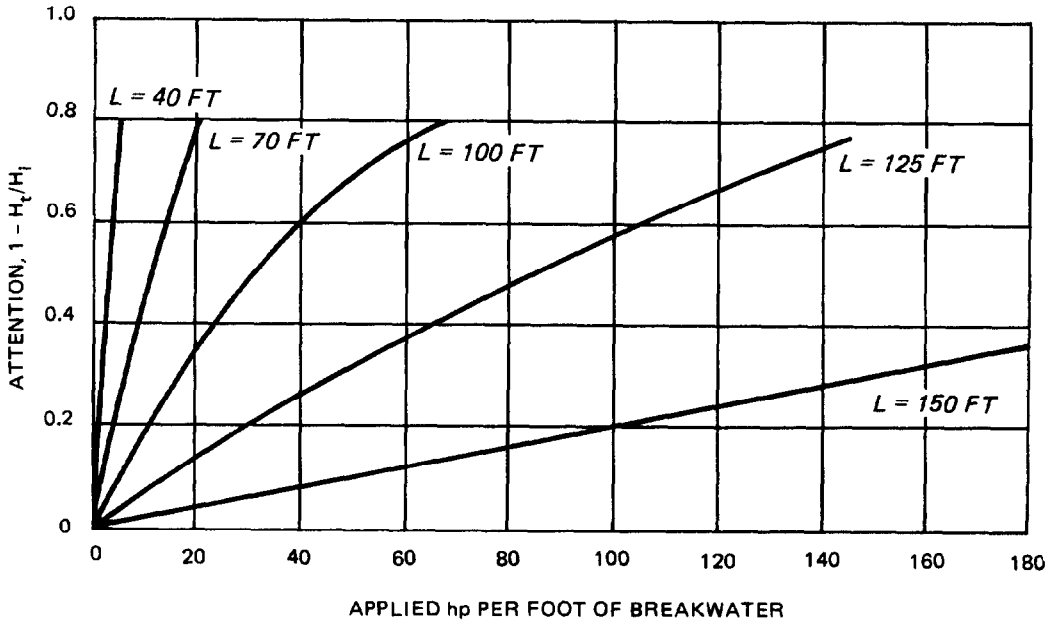

Figure 7-1. Effect of applied horsepower and wavelength L on effectiveness of the pneumatic breakwater at a 40-foot depth

c. Large-Scale Experimental Studies. Pneumatic wave attenuation systems have one distinct advantage in that they allow unrestricted passage over the breakwater. Sherk considered that the concept merited large-scale experimental investigation despite the large horsepower requirements predicted from the previous small-scale tests (item 119). Sherk's experimental study was conducted in 16 feet of water using various wave heights and periods. Wave periods ranged from 2.61 to 16.01 seconds, sufficiently covering the range of wave periods most often found in the open ocean. The larger scale tests indicated that approximately 20 percent less horsepower than was predicted from previous small-scale tests is needed to produce a like attenuation. Operation would still be costly, even with this small reduction in the power requirement.

7-3. Hydraulic Breakwater System. Hydraulic breakwaters achieve wave attenuation by discharging water under pressure through a manifold in a direction opposed to a train of surface gravity waves. The water jets diffuse, a horizontal current is formed, and a high degree of turbulence and mixing

occurs. Waves propagating into the current dissipate a portion of their energy by partial or complete breaking. Thus, the hydraulic breakwater is conceptually similar to the pneumatic breakwater except for the manner in which the horizontal current is formed. Performance of the hydraulic breakwater has been investigated for intermediate depth waves ($0.05 < d/L < 0.5$) (items 60, 125, and 146). The primary objectives of the two-dimensional hydraulic breakwater studies, described in items 60 and 123, were to obtain information concerning the effects of various parameters on wave attenuation, discharge, and horsepower requirements. Experimental data indicated that power requirements primarily depend on wavelength, water depth, and wave steepness, and submergence, spacing, and size of nozzles.

a. Effect of Relative Wavelength. Data were obtained for d/L values ranging from 0.2 to 1.0. For a constant level of attenuation, power requirements remained fairly constant as d/L decreased from 1.0 to 0.5, and then increased rapidly for smaller values of d/L, with the power requirement at $d/L = 0.2$, being seven times greater than that observed for $d/L = 0.5$.

b. Effect of Wave Steepness. Wave steepness was found to have an important effect on power requirements. For a constant level of attenuation and constant d/L, the required horsepower increased by a factor of about three as the incident wave steepness (H_i/L_i) increased from 0.02 to 0.08.

c. Effect of Jet Area. Jet nozzle cross-sectional area per linear foot of breakwater has been found to influence both the discharge and power requirements. Generally, power requirements decrease and the required discharge increases as the jet area is increased.

d. Efficiency. Herbich, Ziegler, and Bowers found that more power was required to attenuate relatively steep waves than flatter waves; however, the efficiency of the system, e, was found to be higher for the steeper waves (item 60). The efficiency e can be defined as

$$e = \frac{(P_i - P_t)}{P_j} \tag{7-4}$$

where

P_i = the power of the incident wave train

P_t = the power of the transmitted wave train

P_j = the power of the hydraulic jets

As illustrated in figure 7-2, efficiency varied with incident wave steepness H_i/L_i, relative wavelength d/L, and attenuation. Assuming an installation

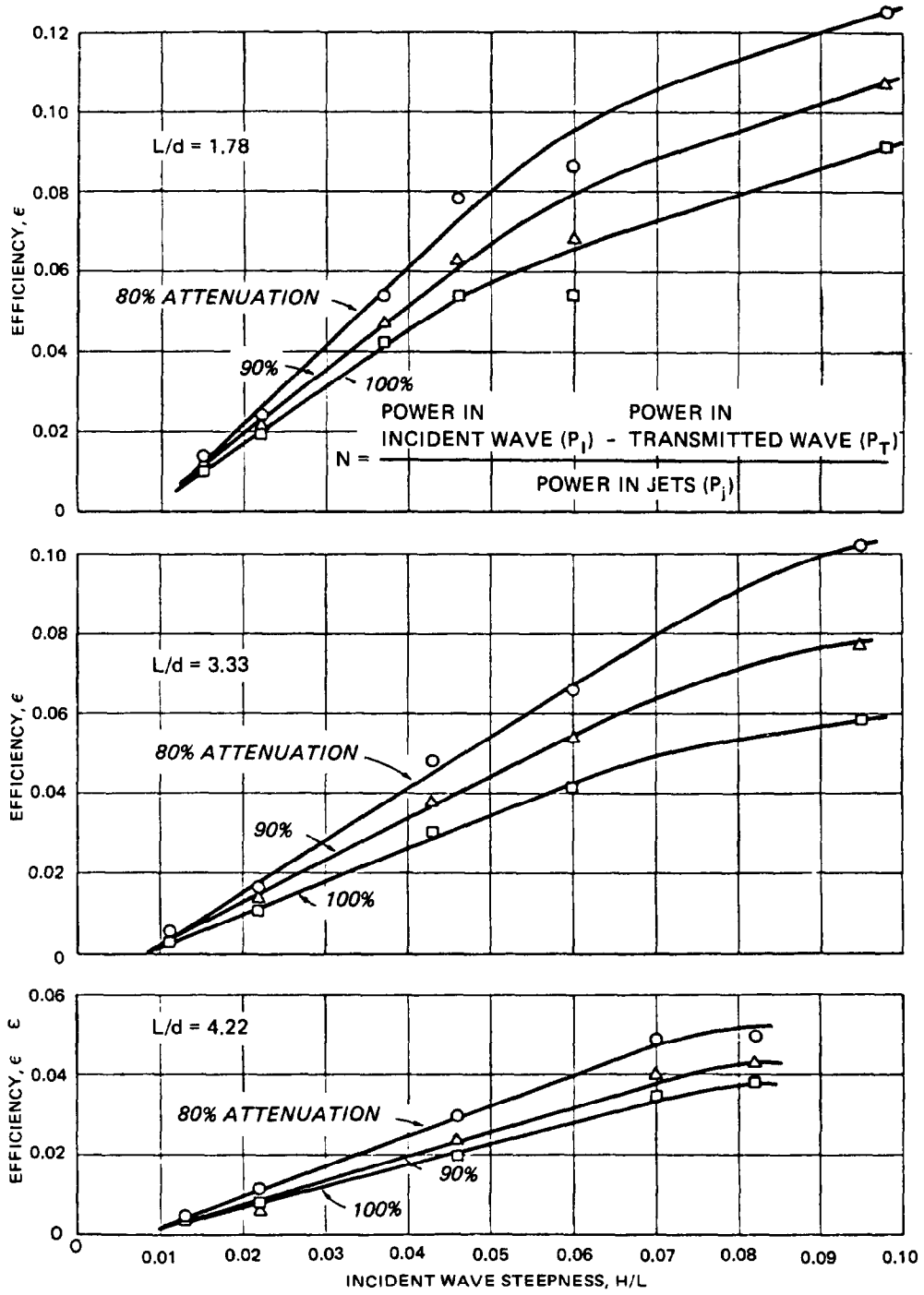

Figure 7-2. Efficiency of the hydraulic breakwater as a function of wave steepness, H/L , and relative wavelength, L/d

depth of 40 feet and for various wave conditions, attenuation as a function of applied horsepower per foot of breakwater is shown in figure 7-3. Similar to the pneumatic breakwater, the hydraulic breakwater's horsepower requirement would make operation very costly. It should be noted that neither the pneumatic nor the hydraulic breakwater have proven cost effective in a prototype installation.

7-4. Sloping Float Breakwater.

a. General. The sloping float breakwater (SFB) is a wave barrier that consists of a row of flat slabs or panels, with weight distribution such that each panel rests with one end above the water surface and the other end on the bottom. Hollow steel barges of the Ammi pontoon or Navy Lightered pontoon type afford one means of construction; however, various other types of construction are possible. Deployment of the pontoon-type structures would consist of assembling unballasted modules at the surface and then partially flooding the barges so that the stern sinks and rests on the bottom and the bow floats above the water surface. The height of protrusion of the bow above the water surface (freeboard) is controlled by flooding a selected number of pontoons. Barges are sited so that the bow faces into the primary direction of wave attack, and mooring lines are attached between it and a bottom anchor. Figure 7-4 is a conceptual sketch of the SFB. Performance of the SFB has been investigated in hydraulic model tests using monochromatic waves (items 107, 109, and 110). Hydraulic model tests of the concept using spectral waves are described in item 30.

b. Wave Attenuation Capabilities.

(1) In hydraulic model tests (item 30) an investigation was conducted of a wide range of wave periods, wave heights, and water depths. Tests were conducted with a 1V:50H bottom slope using shallow-water wave spectra characteristic of the North Carolina coast. Even though tests were site specific, it is felt that they should provide good general guidance to expected SFB performance due to the wide range of conditions investigated and the commonality of shallow-water wave spectra for similar wave heights and periods. Therefore, findings discussed within item 30 are summarized in the following paragraphs.

(2) The SFB's selected for testing were Navy Lightered pontoon-type barges 89.6 and 118.4 feet long, weighing 134,000 and 177,000 pounds, respectively. Both were 21 feet wide and 5 feet deep. Tests were conducted with about 5 feet of freeboard. This condition required 366,000 and 467,000 pounds of seawater ballast for the 89.6- and 118.4-foot barges, respectively.

(3) Important geometric and dynamic details of the prototype barges were considered in the design and construction of the model section. Overall prototype dimensions were exactly reproduced, and all major parameters that control rigid body dynamic response such as weight, center of gravity, mass moments of inertia, and angle of inclination were reproduced within

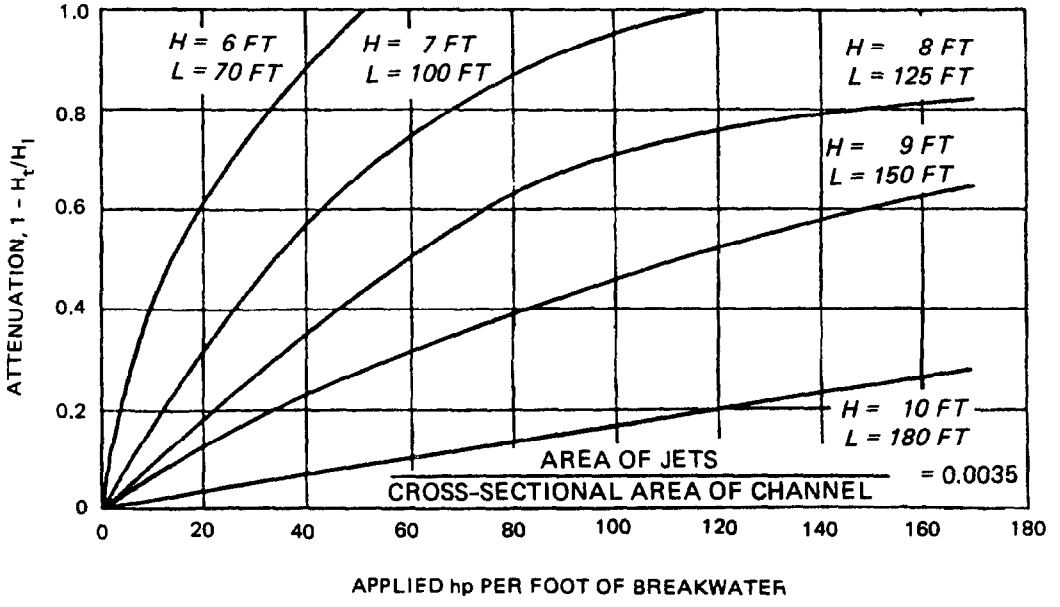

Figure 7-3. Effect of applied horsepower and wavelength, L , on effectiveness of the hydraulic breakwater at a 40-foot depth (H_t = transmitted wave height)

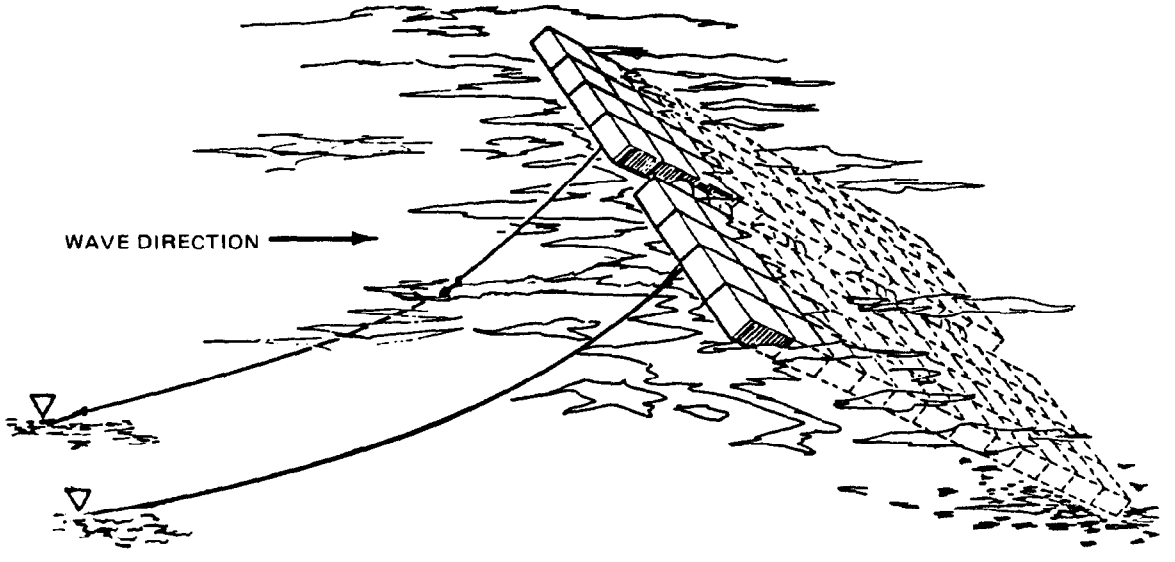

Figure 7-4. An artist's conception of the sloping float breakwater (SFB)

±1.0 percent. Barges were moored to a bottom anchor using a 150-foot-long braided nylon line with a breaking strength of 230,000 pounds. Nonlinear restoring force characteristics of the mooring line were simulated in the model with a series of springs.

(4) All tests were conducted with spectral waves. Peak periods (T_p) of the spectra ranged from 6 to 14 seconds, and the significant wave heights (H_s) were 2, 4, 6, and 8 feet. The structures were anchored in water depths of 13, 15, 18, and 21 feet.

(5) Examination of wave test results from item 30 shows that coefficients of transmission (C_t) and peak mooring force (F_p) appear to primarily depend on wave period or length, SFB length, and water depth, i.e.,

$$C_t = f(T_p, L_{SFB}, d)$$

$$F_p = f(T_p, L_{SFB}, d)$$

The variables T_p, L_{SFB}, and d are defined as the peak period of the spectra, length of the sloping float breakwaters (SFB) and water depth, respectively. Figures 7-5 and 7-6 present C_t and F_p, respectively, as a function of wave period for SFB lengths of 118.4 and 89.6 feet and a water depth of 18 feet. Figures 7-7 and 7-8 present C_t and F_p, respectively, as a function of water depth, for SFB lengths of 118.4 and 89.6 feet and wave periods ranging from 6 to 14 seconds.

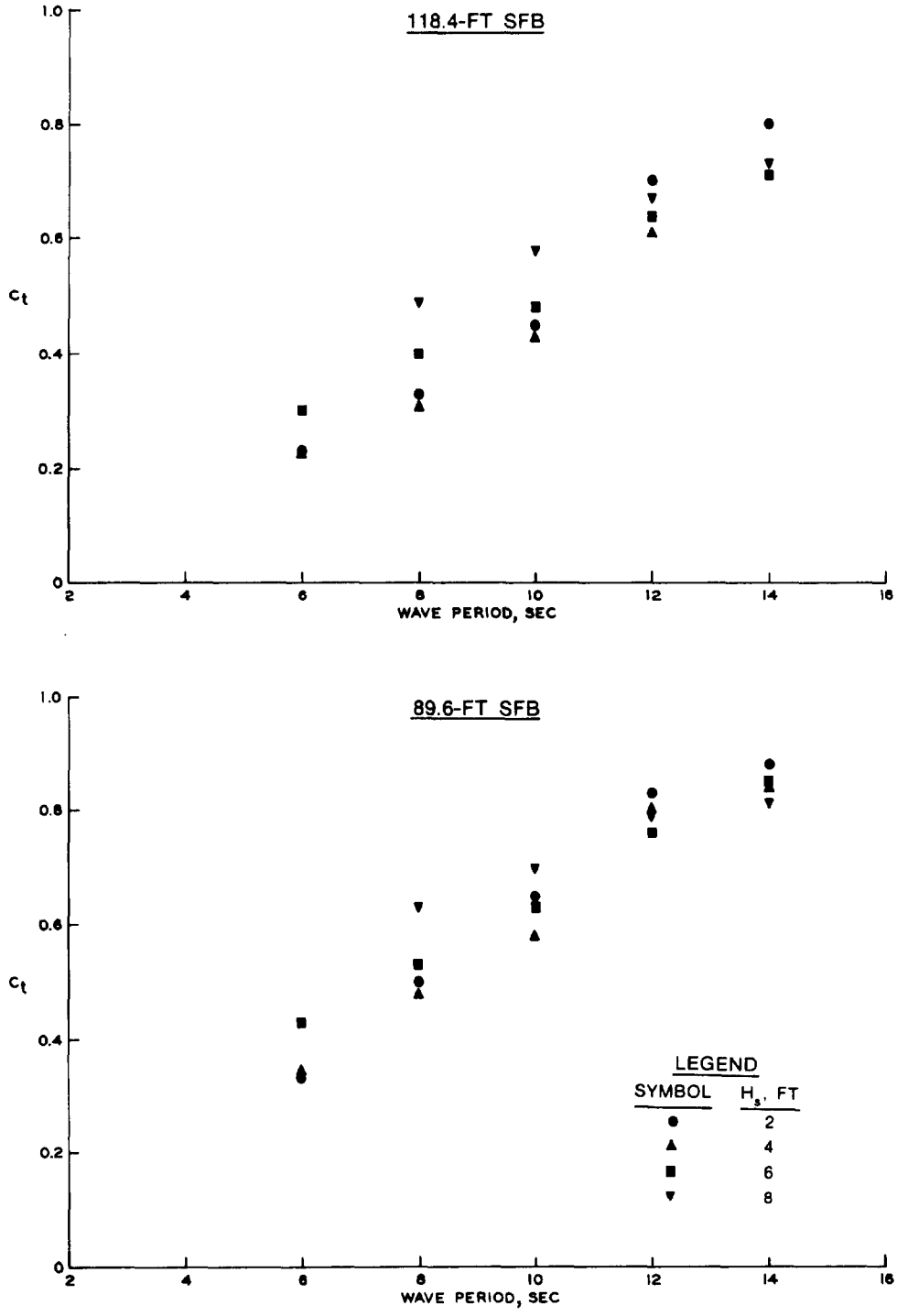

Figure 7-5. Wave attenuating capabilities of the SFB in an 18-foot water depth

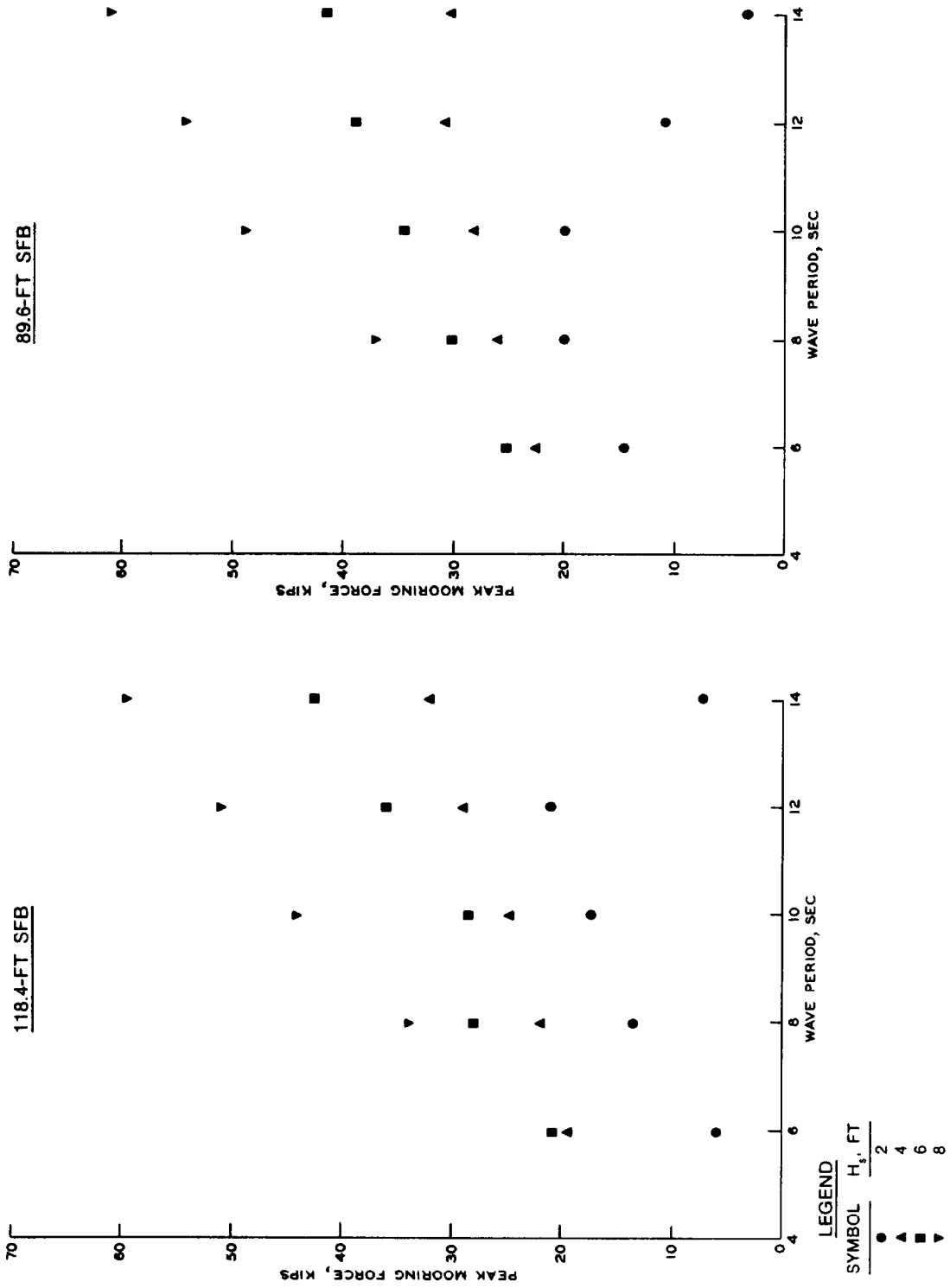

Figure 7-6. Peak mooring forces developed by the SFB in an 18-foot water depth

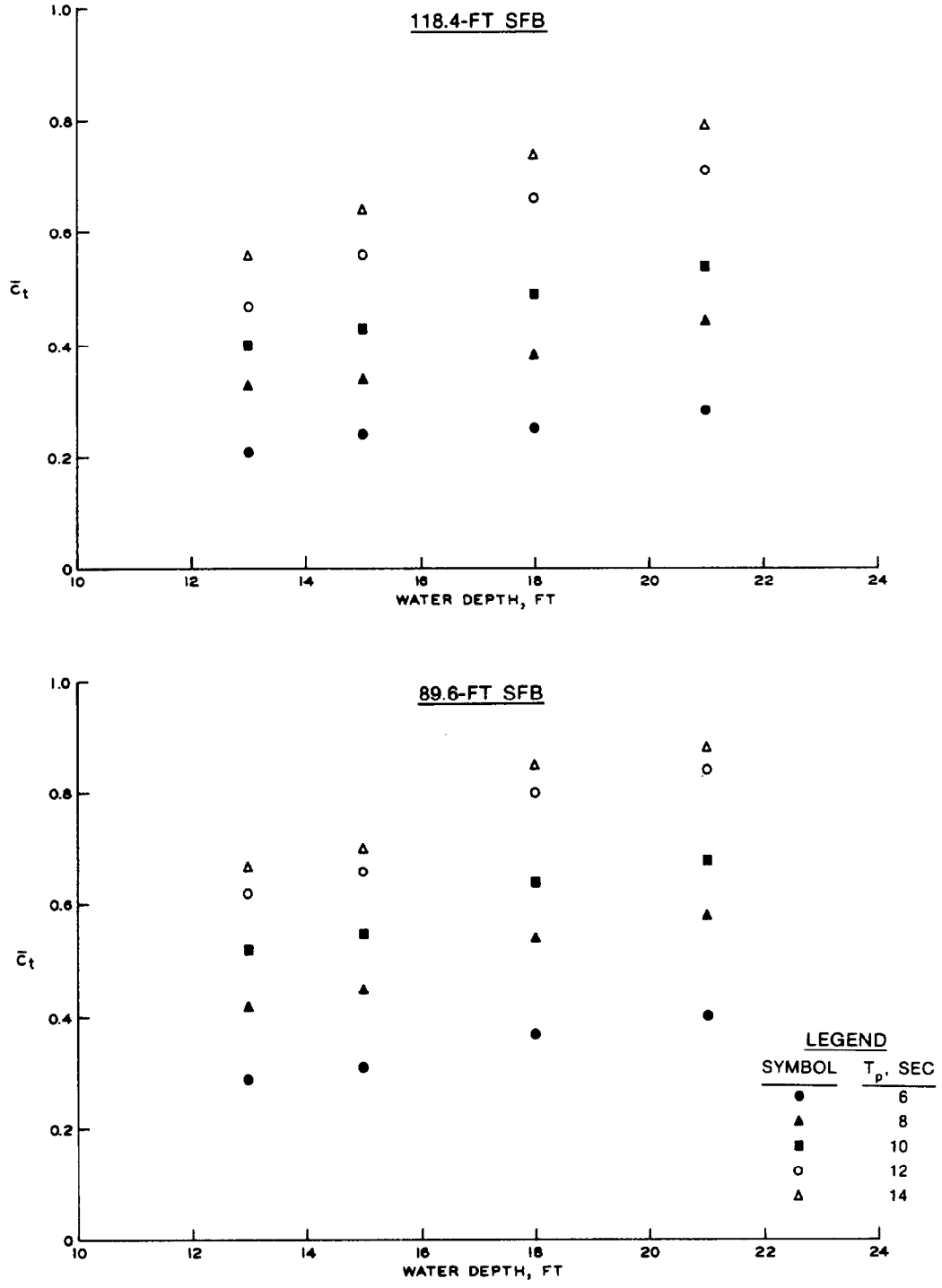

Figure 7-7. Wave attenuating capabilities of the SFB as a function of water depth, wave period, and breakwater length

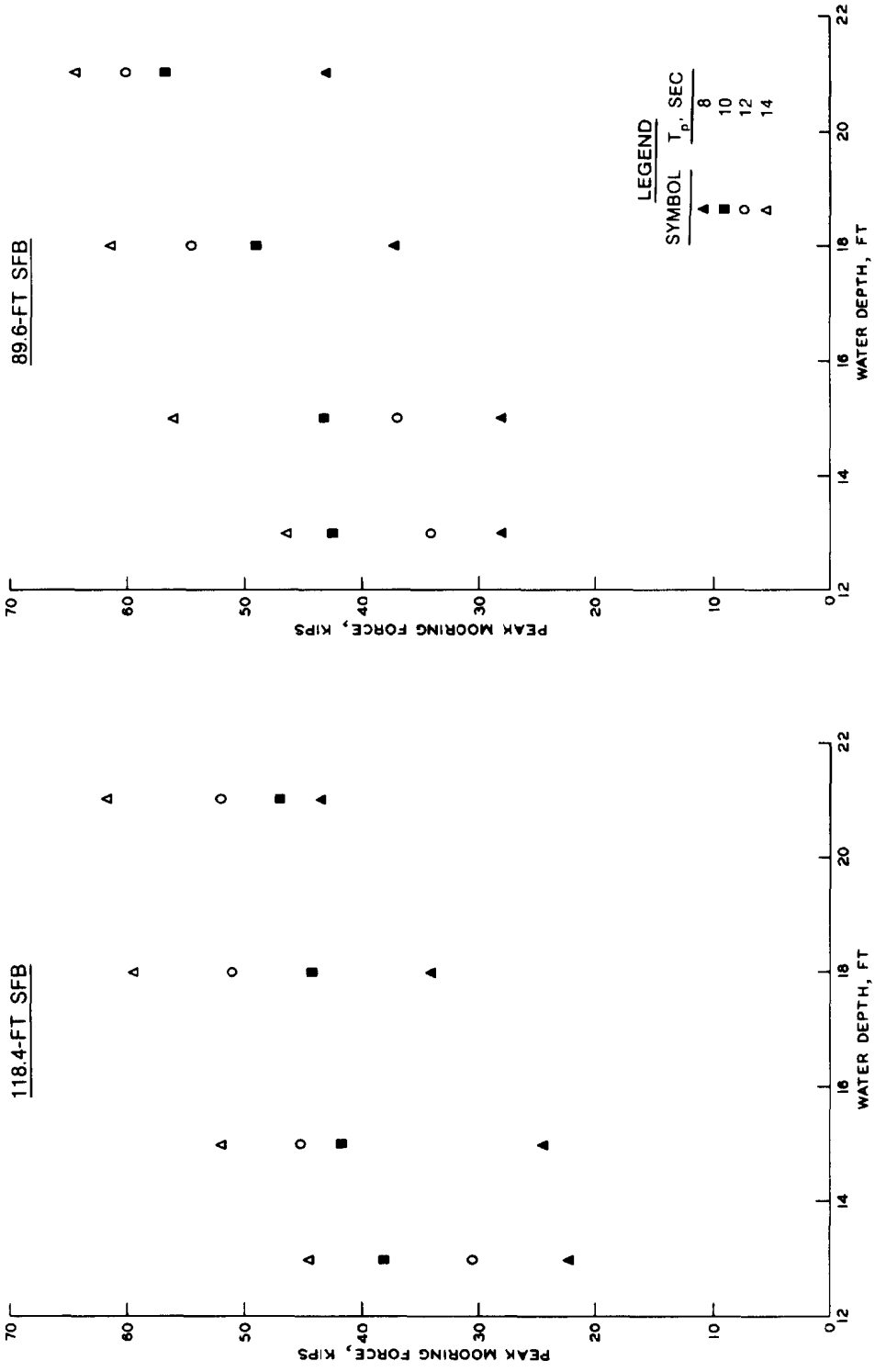

Figure 7-8. Peak mooring forces developed by the SFB under attack of 8-foot waves as a function of water depth, wave period, and breakwater length